Strain Rate Induced Amorphization in Metallic Nanowires

Hideyuki Ikeda,[2,*] Yue Qi,[1] Tahir Çagin,[1] Konrad Samwer,[2,†] William L. Johnson,[2] and William A. Goddard III[1,‡]

[1]*Materials and Process Simulation Center, California Institute of Technology, Pasadena, California 91125*

[2]*Keck Laboratory of Engineering Materials, California Institute of Technology, Pasadena, California 91125*

(Received 10 September 1998)

Using molecular dynamics simulations with a many-body force field, we studied the deformation of single crystal Ni and NiCu random alloy nanowires subjected to uniform strain rates but kept at 300 K. For all strain rates, the Ni nanowire is elastic up to 7.5% strain with a yield stress of 5.5 GPa, far above that of bulk Ni. At high strain rates, we find that for both systems the crystalline phase transforms continuously to an amorphous phase, exhibiting a dramatic change in atomic short-range order and a near vanishing of the tetragonal shear elastic constant perpendicular to the tensile direction. This amorphization which occurs directly from the homogeneous, elastically deformed system with no chemical or structural inhomogeneities exhibits a new mode of amorphization. [S0031-9007(99)08867-5]

PACS numbers: 61.43.Dq, 62.20.Fe, 64.70.Pf, 68.35.Rh

Since their discovery in 1960 the formation and properties of amorphous metal alloys have been of great interest. Generally the strategy for forming amorphous metals involves alloying with elements that are dissimilar in size and bonding (chemical disorder) or by introducing various defects [1] followed by sufficiently rapid decreases in the temperature that there is no time for crystal nuclei to form. In contrast, we show here that *a homogeneous perfect crystal at constant temperature can be transformed continuously to an amorphous metal by application of sufficiently large strain rates.* Thus, there are now three orthogonal processes for forming amorphous metals: (i) Rapid quenching from a liquid. (ii) Introduction of chemical or physical disorder. (iii) Application of rapid strain rates.

We used molecular dynamics (MD) simulations to strain fcc crystalline nanowires at a uniform rate along the $\langle 001 \rangle$ crystallographic direction [2–4]. Here, to realize an infinite nanowire we applied 1D periodic boundary condition in the c direction (an initial length of ten fcc unit cells, $\approx$4 nm, while the a and b directions are five fcc cells long, $\approx$2 nm). We studied the deformation behavior at constant *strain rates* (0.05% to 5% ps^{-1}) and constant temperature (300 K). The tensile strain component ε_{33} was applied uniformly (in increments of 0.5%) to obtain the specified strain rate. The average stress components σ_{ij} in the specimen were computed at and following each applied strain increment. At the strain rates reported here, the stress distribution relaxes between strain increments to a homogeneous stationary equilibrium state of uniaxial tensile stress. We observe a crystal to glass transformation at 300 K above a critical strain rate.

Such large strain rates are observed experimentally only in shock wave and high velocity impact studies, where it has been difficult to control temperature or to obtain details about dynamic structural changes. Experiments at such high strain rates lead to shear localization arising from adiabatic heat dissipation and local thermal softening of the material, which results in highly nonequilibrium systems that are difficult to study experimentally. The MD simulations follow the effects of loading and loading rate independently from those arising from heat dissipation and concomitant temperature increases.

To illustrate the effect of strain rate on the detailed deformation, Fig. 1 displays snapshots of MD simulations on an fcc NiCu random alloy nanowire (at 300 K) deformed to 100% strain at strain rates from 0.5% and 5% ps^{-1} in the z direction.

For $\dot{\varepsilon} = 0.5\%\ ps^{-1}$ cooperative shear events within the crystal produce coherent shear bands, which are often coherent "twins." Multiple coherent shearing events finally lead to necking before failure. For $\dot{\varepsilon} = 5\%\ ps^{-1}$, the behavior is fundamentally different. No coherent shear bands or twins form as the system is strained. Instead, the specimen transforms homogeneously to an amorphous state at strains of only 0.15. This homogeneously disordered material undergoes homogeneous uniform flow as characteristic of a liquid or amorphous solid [5] with no

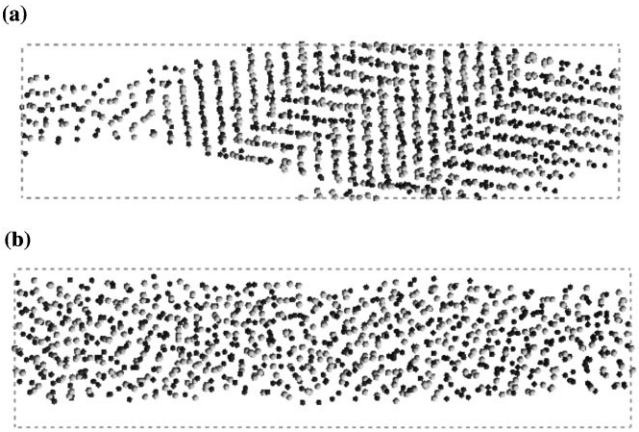

FIG. 1. Snapshots of a fcc NiCu alloy nanowire at 100% strain, deformed at uniform strain rates starting with the random alloy single crystal at 300 K. (a) 0.5% ps^{-1}; (b) 5.0% ps^{-1}.

 0031-9007/99/82(14)/2900(4)$15.00

evidence of the work hardening or necking expected in the crystalline state.

Figure 2 shows how the strain rates affect the stress-strain curves (pure Ni at $T = 300$ K). For all strain rates, the stress increases linearly with strain (ε_{33}) up to $\sim$5.5 GPa and 7.5% strain. This elastic yield stress and yield strain far exceed that of bulk Ni.

Past the elastic limit (7.5% strain), for lower strain rates ($\dot{\varepsilon} = 0.05\%$ or 0.5% ps^{-1}), the stress drops rapidly by 50% (to 2.8 GPa). With further strain, the stress again rises, then drops in a repeating loading/plastic deformation cycle. The sample remains crystalline during these stepwise transitions and accommodates the strain through heterogeneous plastic deformation occurring by formation of cooperatively sheared regions with reoriented fcc crystal (see Fig. 1). Such transformations have been observed previously in plastic deformation of crystals, and were explained in terms of twin formation or similar cooperative shear processes [6].

For $\dot{\varepsilon} = 5\%$ ps^{-1}, Fig. 2 shows a very different behavior. Beyond 7.5% strain, the system changes continuously from a fcc crystal to a glass with accompanying homogeneous plastic flow. Thus, there is a gradual rounding of the stress-strain curve with none of the "twinning related" stress drops observed at lower strain rates. The maximum stress of $\sigma_{33} = 9.5$ GPa occurs at $\sim$15% strain (Ni at 300 K). Further plastic deformation leads to decreased stress, with a limiting value of $\sigma_{33} \sim 3$ GPa and a calculated viscosity ($\sigma_{33}/\dot{\varepsilon}$) of $\eta \sim 0.60$ poise. Even at this high strain rate, the sample is homogeneous with a normal Poisson contraction in the ε_{11} and ε_{22} strains and no localized shear events.

Figure 3(a) shows that for $\dot{\varepsilon} = 0.5\%$ ps^{-1} the maxima in the radial distribution function (RDF), $G(r)$, expected for a crystalline fcc system remain for distances up to 0.55 nm, but broaden. In particular, the second nearest neighbor peak around 0.32 nm of fcc structure is clearly resolved.

Figure 3(b) shows the RDF for Ni as a function of strain for $\dot{\varepsilon} = 5\%$ ps^{-1}. At $\varepsilon = 0.1$ the RDF still shows the peak near 0.32 nm representing the octahedral sites, but for $\varepsilon = 0.15$ this peak is gone. Thus, for strains above 0.15 the RDF suggests that the crystalline phase has transformed to the amorphous phase. However, starting with the amorphous state achieved at a strain of $\varepsilon = 0.2$ from straining at 5% ps^{-1} and then slowing the strain rate to 1% ps^{-1}, we found that the sample recrystallizes. Thus, for pure Ni at 300 K the critical strain rate to transform and remain amorphous is close to 5% ps^{-1}.

Figure 4 shows the elastic constants for Ni as a function of strain for $\dot{\varepsilon} = 5\%$ ps^{-1}. The uniaxial tension in the z direction breaks the cubic symmetry so that the three independent elastic constants split into six independent elastic constants for the tetragonal system: $C_{11} = C_{22}$, C_{33}, C_{12}, $C_{13} = C_{23}$, $C_{44} = C_{55}$, and C_{66}. By a strain of 0.4 to 0.7 we observe the four independent elastic constants: $C_{11} = C_{22}$, C_{33}, $C_{12} = C_{13} = C_{23}$, $C_{44} = C_{55} = C_{66}$ expected for a homogeneous amorphous glass under steady state uniaxial deformation, in particular, $C_{66} = (C_{11} - C_{12})/2$, as for an isotropic solid. Thus, Fig. 4 indicates that the amorphization process starts at 10% strain but is not complete

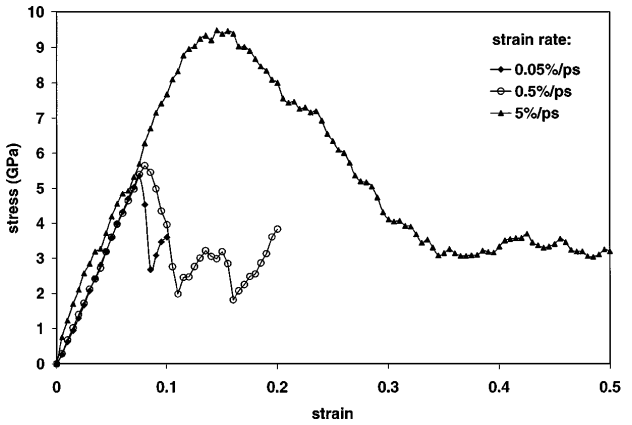

FIG. 2. Stress-strain curves for strain rates of 0.05% to 5% ps^{-1} starting with a pure Ni nanowire crystal at $T = 300$ K. All three strain rates show elastic behavior up to $\sim$7.5% strain. For 0.05% and 0.5% ps^{-1} the stress is relaxed by twin formation, which subsequently hardens the material, leading to a zigzag stress-strain curve. For 5% strain rate there is a continuous transformation to the amorphous phase of pure Ni.

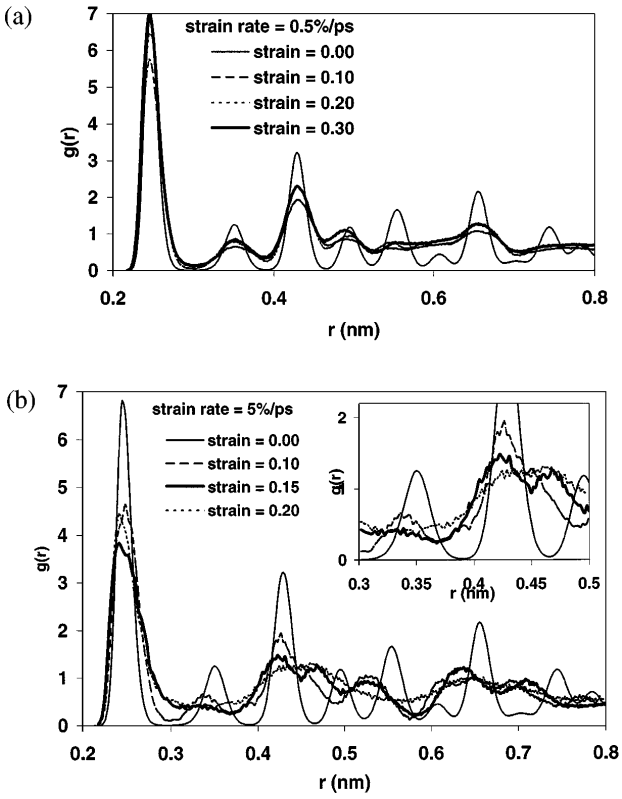

FIG. 3. Radial distribution function of Ni nanowires for various strains at strain rates of (a) 0.5% ps^{-1}; (b) 5.0% ps^{-1}.

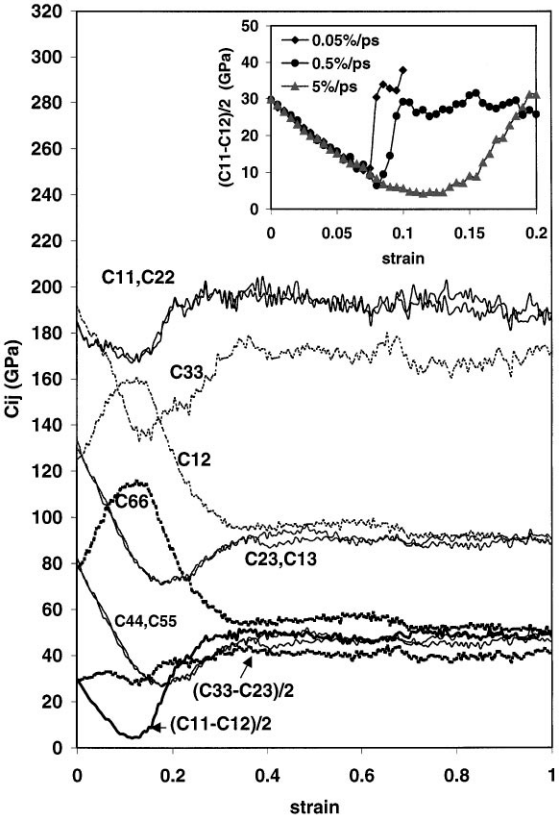

FIG. 4. Elastic constants for the Ni nanowire for a strain rate of 5% ps^{-1} (at 300 K). The strain (in the z direction) leads to six independent C_{ij} ($C_{11} = C_{22}$, C_{33}, C_{12}, $C_{13} = C_{23}$, $C_{44} = C_{55}$, and C_{66}). The tetragonal shear in the xy plane, $(C_{11} - C_{12})/2$, goes toward zero at the critical point (0.11 strain) for transforming to the amorphous phase. The steady state amorphous phase in uniaxial tension (above $\sim$ 0.6 strain) has four independent constants. The inset shows $C_{11} - C_{12}$ for lower strain rates.

until 40%–70% strain (where we find the expected symmetry related degeneracies in the C_{ij}'s). Thus, this relaxation takes $\sim$6 to 12 ps, corresponding to the time for a shear wave to traverse the MD cell a few times.

The inset of Fig. 4 shows that the tetragonal shear modulus in the xy plane, $(C_{11} - C_{12})/2$, decreases linearly with increasing strain for all strain rates (pure Ni at $T =$ 300 K) up to $\sim$7.5% strain. However, for $\dot{\varepsilon} \leq 0.5\%$ ps^{-1}, the shear modulus suddenly increases at 7.5% strain state back to its original value. This is due to the relaxation of stress by twinning or coherent shearing (Fig. 2). The linear extrapolation of $(C_{11} - C_{12})/2$ to zero would predict a vanishing shear modulus at 11% strain. Such a vanishing of the shear rigidity is associated with the solid to liquid transformation [7(a)] [either [7(b)] the rhombohedral shear modulus (C_{44} for cubic) or the tetragonal shear modulus ($C_{11} - C_{12}$ for cubic)]. Tallon [8] showed that the shear moduli do *not* vanish at the thermodynamic melting temperature T_m. Rather they decrease with increasing temperature in such a way as to extrapolate to zero at a critical temperature above T_m. He also found that this instability is triggered by the vanishing of $(C_{11} - C_{12})/2$ rather than C_{44}. Recently, Wang *et al.* [9] derived modified stability conditions for the case of strained solids by including the hydrostatic pressure into the strain tensor, which becomes important close to the instability. The vanishing of elastic constants near the crystal to glass transition has been measured experimentally [10–14].

For $\dot{\varepsilon} = 5\%$ ps^{-1} strain rate, we find no sudden increase of the tetragonal shear modulus $(C_{11} - C_{12})/2$. Instead it decreases with increasing strain, first linearly, then less rapidly as it approaches the critical condition. It continues to decrease until the strain is $\sim$10%, then bends to form a minimum at 12% strain and then finally increases to a limiting value after 30% as the amorphization transition is complete. The deviation from a linear extrapolation from 10% to 12% strain is, we believe, related to the presence of critical shear fluctuations as the system approaches the $(C_{11} - C_{12})/2 = 0$ condition. Figure 4 shows that the rhombohedral shear moduli $C_{44} = C_{55}$ extrapolate to vanish at a strain of 20%, much higher than for the tetragonal shear (11%), as suggested by Tallon [7]. Although the tetragonal shear modulus in the x-y plane nearly vanishes at 11% strain, the tetragonal shear modulus in xz and yz planes, $(C_{33} - C_{23})/2$, increase. Thus, the fcc nanowire first begins to amorphize in the xy plane.

The limiting viscosity of $\eta = 0.06$ poise calculated from Fig. 2, combined with the limiting shear stress of $G_0 = (C_{11} - C_{12})/2 = 50$ GPa from Fig. 4, combined with the Maxwell relation, $\eta = G_0\tau$, suggests a relaxation time of $\tau = 1.2$ ps. This corresponds to 6% strain in Fig. 4, which is consistent with the observed relaxation time for the stresses in the amorphous phase.

In conclusion, we report that strain rate can induce amorphization/melting in homogeneous elastically strained fcc single crystal nanowires. This transformation is indicated by the following: (i) the change in the RDF expected for an amorphous material (loss of the second-nearest-neighbor peak at 0.32 nm); (ii) the symmetry in the elastic constants $[C_{66} = (C_{11} - C_{12})/2]$ expected for an amorphous material and (iii) the vanishing tetragonal shear modulus $[(C_{11} - C_1)/2 \rightarrow 0]$ at the start of the transformation; (iv) a limiting stress for uniform strain rate (leading to a viscosity of 0.06 poise). Effectively the strain rate of $\dot{\varepsilon} = 5\%$ ps^{-1} has decreased the melting temperature down to less than 300 K (the calculated and experimental values for the crystalline phase are $\sim$1700 K). For pure Ni and NiCu alloys we find that the critical strain rate for the crystal to glass transition is below 5% ps^{-1}. For strain rates of 0.5% ps^{-1} and less, we find cooperative shear events (twins) in the nanowire but no phase transitions.

Financial support was provided by the Japanese Ministry of Education for H. I., by DOE (DEFOG3 86ER45242) for K. S. and W. L. J., by ARO (DAAH04-95-1-0233) for W. L. J. and W. A. G., and by NSF (CHE

95-22179 and ACR-92-17368) and DOE-ASCI for Y. Q., T. C., and W. A. G. In addition, the facilities of the MSC are supported by grants from ARO-DURIP, BP Chemical, Exxon, Avery-Dennison, Owens-Corning, ARO-MURI, Asahi Chemical, Chevron Corp., and Beckman Institute.

*Current address: Department of Mechanical Engineering, Kagoshima National College of Technology, Kagoshima 899-5193, Japan.

†Current address: Institut für Physik, Universität Augsburg, D-86135 Augsburg, Germany.

‡To whom correspondence should be addressed. Email address: wag@wag.caltech.edu

[1] K. Samwer, H. Fecht, and W. L. Johnson, in *Glassy Metals III,* edited by H. Beck and H. J. Guntherodt (Springer, Berlin, 1994). We note here that there are other examples of homogeneous amorphization which is observed in materials such as GaAs, $GeSe_2$ [see Z. W. Popovic, Y. S. Raptis, E. Anastassakis, and Z. Jackiw, J. Non-Cryst. Solids B **230**, 794 (1998)] and in minerals [for a recent review see P. Richet and P. Gillet, Eur. J. Mineral. **9**, 907 (1997)] due to applied pressure.

[2] The MD simulations use the quantum Sutton-Chen (Q-SC) force field [3(a)] to model the atomic interactions of the pure metals (Au, Cu, and Ni) and their alloys (Cu-Ni and Au-Ni). This force field leads to accurate thermodynamic and transport properties for metals and alloys [3(b)–3(e)]. Before deformation, the sample was allowed to relax at 300 K for 110 ps but with the sample length fixed. Using the coordinates of the unstressed infinite cubic system for the wires leads to initial stress components of $\sigma_{33} = 1.9$ GPa, $\sigma_{11} = -0.1$ GPa, and $\sigma_{22} = -0.1$ GPa. This arises from the capillary forces associated with the free surfaces. $F_Z = \partial E_s/\partial L = (\partial/\partial L)(4\gamma\sqrt{V_0/L}\,L)$. We calculate the total surface tension to be $\sigma_{\mathrm{cap}}^{33} = F_z/(V_0/L) = (2\gamma/\sqrt{V_0})L^{1/2}\gamma = 1\ \mathrm{J/m^2}$, which is comparable to experimental values for Ni, Cu [4].

[3] (a) Y. Kimura, T. Çagin, Y. Qi, and W. A. Goddard III (to be published). See also A. P. Sutton and J. Chen, Philos. Mag. Lett. **61**, 139 (1990); (b) Y. Qi, T. Çagin, Y. Kimura, and W. A. Goddard III, Phys. Rev. B **59**, 3527 (1999); (c) Y. Qi, T. Çagin, Y. Kimura, and W. A. Goddard (to be published); (d) G. Dereli, T. Çagin, M. Ulodogan, and M. Tomak, Philos. Mag. Lett. **75**, 209 (1997); (e) T. Çagin, G. Dereli, M. Ulodogan, and M. Tomak, Phys. Rev. B **59**, 3468 (1999).

[4] R. A. Swalin, *Thermodynamics of Solids* (Wiley, New York, 1962).

[5] L. Davis, in *Metallic Glasses*, edited by J. J. Gilman and H. Leamy (ASM International, Metals Park, OH, 1978), Chap. 8.

[6] T. Kitamura, K. Yashiro, and R. Ohtani, JSME Int. J. A, Mech. Mater. Eng. **40**, 430 (1997).

[7] (a) M. Born, J. Chem. Phys. **7**, 591 (1939). (b) M. Born, Proc. Cambridge Philos. Soc. **36**, 160 (1940).

[8] J. L. Tallon, Nature (London) **342**, 658 (1989).

[9] J. Wang, J. Li, S. Yip, D. Wolf, and S. Phillpot, Physica (Amsterdam) **240A**, 396 (1997).

[10] C. Ettl and K. Samwer, Mater. Sci. Eng. A **178**, 245 (1994).

[11] R. Hassdorf, M. Arend, and W. Felsch, Phys. Rev. B **51**, 8715 (1995).

[12] P. R. Okamoto *et al.,* J. Less-Common Met. **140**, 231 (1988).

[13] J. Chevrier and J. B. Suck, Phys. Rev. B **49**, 961 (1994).

[14] U. Herr, Mater. Sci. Rep. (to be published).